Published in final edited form as:

J Am Chem Soc. 2007 February 14; 129(6): 1524–1525. doi:10.1021/ja0680820.

Fluorescent Core–Shell Ag@SiO_2 Nanocomposites for Metal-Enhanced Fluorescence and Single Nanoparticle Sensing Platforms

Kadir Aslan[†], **Meng Wu**[‡,§], **Joseph R. Lakowicz**[‡], **Chris D. Geddes**[†,‡]

[†]University of Maryland Biotechnology Institute.

[‡]University of Maryland School of Medicine.

[§]Current Position: Department of Neuroscience and High Throughput Biology Center, School of Medicine, Johns Hopkins University, Baltimore, MD 21205.

The use of fluorescent nanoparticles as indicators in biological applications such as imaging and sensing has dramatically increased since the 1990s.[1] These applications require that the fluorescent nanoparticles are monodisperse, bright, photostable, and amenable to further surface modification for the conjugation of biomolecules and/or fluorophores. Among the many types of fluorescent nanoparticles available today, nanoparticles with core–shell architecture fulfill all these requirements, combining diverse functionalities into a single hybrid nanocomposite.[2]

In this work, we have developed core–shell (silver core–silica shell) nanoparticles with various shell thicknesses featuring a variety of fluorophores, to show the versatility of the core–shell architecture, and have demonstrated their applicability for two platform technologies, metal-enhanced fluorescence (MEF) and single nanoparticle sensing. We demonstrate the broad potential applications of our technology by employing near-infrared emitting probes (Rh800) for potential applications in cellular imaging and the use of highly photostable long lifetime (μS) lanthanide probes, probes suitable for off-gating biological autofluorescence. The use of Alexa 647 serves to demonstrate that fluorophores can be readily covalently linked to the core–shell particles also, for metal-enhanced benefits.

MEF is an established technology,[3a-d] where the interactions of fluorophores with metallic nanoparticles results in fluorescence enhancement, increased photostability, decreased lifetime owing to increased rates of system radiative decay, reduced blinking in single molecule fluorescence spectroscopy,[3b] and increased transfer distances for fluorescence resonance energy transfer.[3c] Single-molecule fluorescence spectroscopy is the prime tool in single nanoparticle sensing, and it provides several advantages over ensemble measurements, such as, the elimination of averaging of the spectral properties over all members of the ensemble, which can reveal fundamental features otherwise masked in

geddes@umbi.umd.edu.

Supporting Information Available: The experimental conditions for the preparation of fluorescent core–shell Ag@SiO_2 nanoparticles, nanobubbles, and for TEM, steady-state and single molecule fluorescence spectroscopy. This material is available free of charge via the Internet at http://pubs.acs.org.

ensemble experiments.[4] Accordingly, the use of fluorescent core–shell nanocomposites with single-molecule fluorescence spectroscopy is likely to enhance the capability of single nanoparticle sensing enormously.

The preparation of fluorescent core–shell $Ag@SiO_2$ nanocomposites was undertaken in three steps (see Supporting Information for details): (1) first, silver colloids are prepared by reduction of silver nitrate by sodium citrate, (2) then a silica shell of various thickness was grown on the colloids, and (3) last, fluorophores (i) (Eu-TDPA, [Tris(dibenzoylmethane) mono(5-amino phenanthroline)europium] or Rh800, Rhodamine 800) were doped or (ii) were covalently linked to the silica shell (Alexa Fluor 647). Figure 1 shows the TEM images of core–shell $Ag@SiO_2$ nanocomposites with different thickness of the SiO_2 coating. The diameter of the silver core was 130 ± 10 nm for all the preparations, a size which has been shown suitable for MEF and the radiating plasmon model.[3d] The thickness of the silica shell was varied from 2 to 35 ± 1 nm, to optimize fluorescence enhancement and was controlled by the concentration of tetraethoxysilane (TEOS) after alkaline initiation. The surface plasmon resonance peak for silver shifted toward longer wavelengths as the thickness of the silica shell increased (see Table S1, Supporting Information) as expected and observed by others.[5] The importance of using the silica shell around the silver core is 3-fold: (1) silica layers offer the robustness, chemical inertness, and the versatility needed for the conjugation of biomolecules or fluorophores, (2) it protects the silver core from ions present in biological media, and (3) it allows for the distance dependent MEF phenomenon, which we have determined optimum for shell thicknesses <10 nm.[3d]

To show the “huge” benefits of using a silver core in the fluorescent core–shell nanoparticles, rather than doping the fluorophores directly onto silica nanoparticles without a silver core, as many other researchers have done,[2] we have prepared control sample probes *without* the silver core. The control fluorescent probes, subsequently named hollow fluorescent *nanobubbles*, are prepared by dissolving the silver core away (etching) with cyanide from the fluorescent $Ag@SiO_2$ nanocomposites. Since the fluorophores (Eu-TDPA and Rh800)[6] employed here are hydrophobic and retained in the hydrophobic pockets of the silica shell or covalently linked to the silica shell (Alexa 647), the etching of the silver core with cyanide did not cause the removal of fluorophores from the shell (thickness >10 nm). Thus, it is possible to compare the fluorescence emission and lifetime of the fluorescent core–shell $Ag@SiO_2$ nanocomposites and of the fluorescent nanobubbles in a *quantitative* manner.

It is important to note that the versatility of the preparation technique employed here, allows researchers to incorporate any hydrophobic fluorophore to the silica shell by simply doping fluorophores or by covalently linking those available with suitable amine-reactive groups. Hence, our generic approach allows the use and the benefits of MEF with numerous fluorophores, but in an attractive nanoparticle architecture.

Figure 2 shows the fluorescence emission intensity from Eu-TDPA-doped $Ag@SiO_2$ and Rh800-doped $Ag@SiO_2$ and from the corresponding fluorescent nanobubbles (control samples), Eu-TDPA-doped SiO_2 and Rh800-doped SiO_2. The emission intensity was approximately *8-fold* and *20-fold* higher for Eu-TDPA-doped $Ag@SiO_2$ and Rh800-doped

$Ag@SiO_2$ than for Eu-TDPA-doped SiO_2 and Rh800-doped SiO_2, respectively. We also note that the fluorescence emission spectra of the fluorophores were identical in both cases, indicating that the spectral properties of the fluorophores were retained.

We have also observed that fluorescent core–shell nanoparticles, Rh800 $Ag@SiO_2$, have a faster decay (0.093 ns) than the corresponding nanobubbles (0.447 ns) and the fluorophore in solution (0.728 ns), (see Figure S3 and Table S2 in Supporting Information). The average lifetimes of Alexa 647-linked $Ag@SiO_2$, the corresponding Alexa 647 nanobubble, and Alexa 647 in the aqueous solution were 0.64, 1.73, and 1.05 ns, respectively. These observations are in accordance with the previously described MEF phenomenon [3,7] where the metal–fluorophore interactions result in an increase in the quantum yield (i.e., emission intensity) of the fluorophore and a *decrease* in the lifetime of fluorophores owing to two phenomena: an enhanced local electric field and an increase in the intrinsic system decay rate. The first factor provides stronger excitation rates but does not modify the fluorescence lifetime of the molecules. The second factor increases the net nanoparticle quantum yield.

It is interesting to comment on the total detectability of the new MEF nanoparticles, as this is paramount in microscopy and in single molecule studies. While a 20-fold increase in fluorescence/luminescence intensity is clearly beneficial, a reduced particle lifetime also enables the particle to be cycled faster, as the lifetime of a species determines its cyclic rate. Hence, 20-fold increase in intensity coupled with a 10-fold reduction in fluorophore-particle lifetime, provides for a ~200-fold potential increase in particle detectability. In addition, a reduced lifetime, affords for increased fluorophore photostability,[7-10] as there is less time for excited state photodestructive processes to occur.

Finally, Figure 3 shows representative scanning confocal images of individual fluorescent core–shell nanoparticles, Alexa 647 $Ag@SiO_2$ (covalently linked), and the corresponding nanobubbles, Alexa 647 $@SiO_2$. The bright spots in Figure 3a represent fluorescence emission from the single fluorescent core–shell nanoparticles, while the dimmer spots in Figure 3b,c represent the single nanobubbles. The significant differences in the peak intensities of the two images are immediately evident from Figure 3. For fluorescent core–shell nanoparticles the average value of the peak intensity was approximately 10-fold higher than that of the nanobubbles. This shows that using a silver core results in 10-fold enhancement in the fluorescence emission, which is attributed to the MEF phenomenon.[5] The heterogeneity in the spots' brightness (Figure 3a) is due to the presence of nanobubbles in the same sample as fluorescent core–shell nanoparticles which were not completely separated after the preparation.

In conclusion, we report the development of highly versatile highly fluorescent core–shell $Ag@SiO_2$ nanocomposites, which allow researchers to incorporate any fluorophore to the outer-silica shell by two simple methods (i.e., simple doping or covalent attachment) while exploiting the benefits of using a silver core for MEF. To show the generality of the preparation technique, we have developed three different fluorescent probes: an organic fluorophore (Rh800) and a lanthanide probe doped (noncovalently linked), and another organic fluorophore (Alexa 647) covalently linked to the silica shell. When compared to the control sample fluorescent nanoparticles (nanobubbles), fluorescent nanoparticles with core–

shell architecture yielded up to 20-fold (with Rh800) enhancement of the fluorescence signal and a potentially 200-fold increase in particle detectability.

Supplementary Material

Refer to Web version on PubMed Central for supplementary material.

Acknowledgment.

This work was supported by the National Center for Research Resources, Grant RR008119. Salary support to K.A. and C.D.G. from UMBI is also acknowledged. Authors would like to thank Drs. J. Zhang, J. Lukomska and S. Makowiec for their help with the TEM images and SMFS measurements, respectively.

References

(1) (a). Bruchez M Jr.; Moronne M; Gin P; Weiss S; Alivisatos AP Science 1998, 281, 2013–2016. [PubMed: 9748157] (b)Chan WCW; Nie S Science 1998, 281, 2016–2018. [PubMed: 9748158]

(2) (a). Ow H; Larson DR; Srivastava M; Baird BA; Webb WW; Wiesner U Nano Lett. 2005, 3 (1), 113–117.(b)Gong J-L; Jiang J-H; Liang Y; Shen G-L; Yu R-Q. J. Coll. Inter. Sci 2006, 298, 752–756.(c)Wang L; Yang C; Tan W Nano Lett. 2005, 3, 37–43.

(3) (a). Aslan K; Gryczynski I; Malicka J; Matveeva E; Lakowicz JR; Geddes CD Curr. Opin. Biotechnol 2005, 16, 55. [PubMed: 15722016] (b)Ray K; Badugu R; Lakowicz JR J. Am. Chem. Soc 2006, 128, 8998–8999. [PubMed: 16834349] (c)Malicka J; Gryczynski I; Kusba J; Lakowicz JR Biopolymers 2003, 70, 595. [PubMed: 14648769] (d)Aslan K; Leonenko Z; Lakowicz JR; Geddes CD J. Fluoresc 2005, 13, 643–654.

(4). Michalet X; Pinaud F; Lacoste TD; Dahan M; Bruchez MP; Alivisatos AP; Weiss S Single Mol. 2001, 2, 261.

(5). Kobayashi Y; Katakami H; Mine E; Nagao D; Konno M; Liz-Marzan LM J. Coll. Inter. Sci 2005, 283 (2), 392–396.

(6). Geddes CD Meas. Sci. Technol 2001, 12, R53.

(7). Aslan K; Geddes CD Anal. Chem 2005, 77 (24), 8057. [PubMed: 16351156]

(8). Aslan K; Lakowicz JR; Geddes CD Anal. Bioanal. Chem 2005, 382, 926. [PubMed: 15937664]

(9). Geddes CD; Lakowicz JR J. Fluoresc 2002, 12, 121.

(10). Aslan K; Badugu R; Lakowicz JR; Geddes CD J. Fluoresc 2005, 13 (2), 99–104.

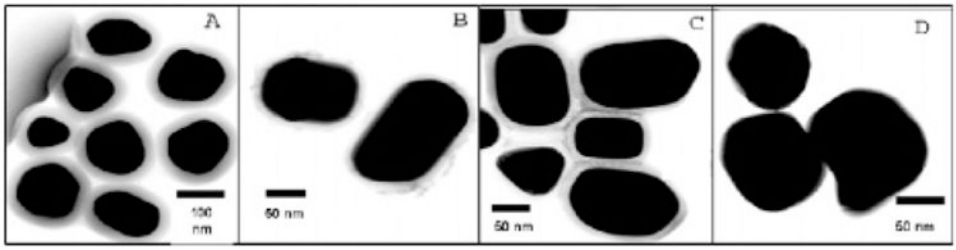

Figure 1.

TEM images of Ag@SiO_2. Panels A, B, C, and D show the samples with different thickness of the SiO_2 coating at 35, 15, 11, and 2 nm (±1 nm), respectively. The diameter of the Ag is 130 ± 10 nm for all the samples.

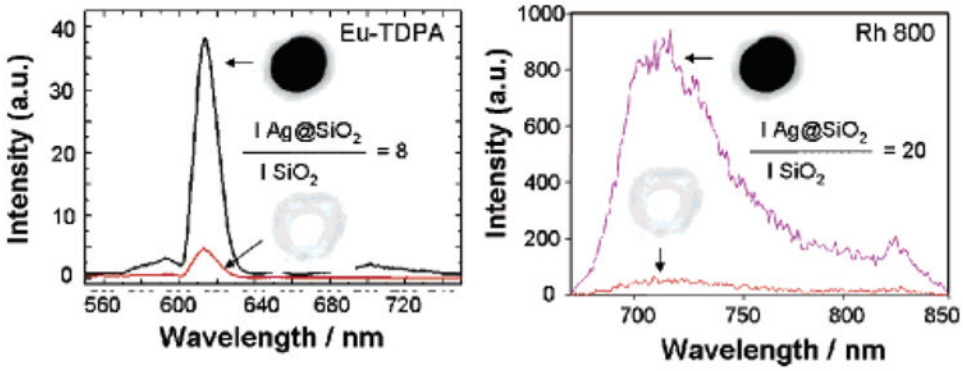

Figure 2.

Fluorescence emission intensity of Eu-TDPA-doped Ag@SiO_2 and Rh800-doped Ag@SiO_2 and from the corresponding fluorescent nanobubbles (control samples), Eu-TDPA-doped SiO_2 and Rh800-doped SiO_2. The diameter of the Ag is 130 ± 10 nm and the thickness of the shell is 11 ± 1 nm (optimized) for all the samples.

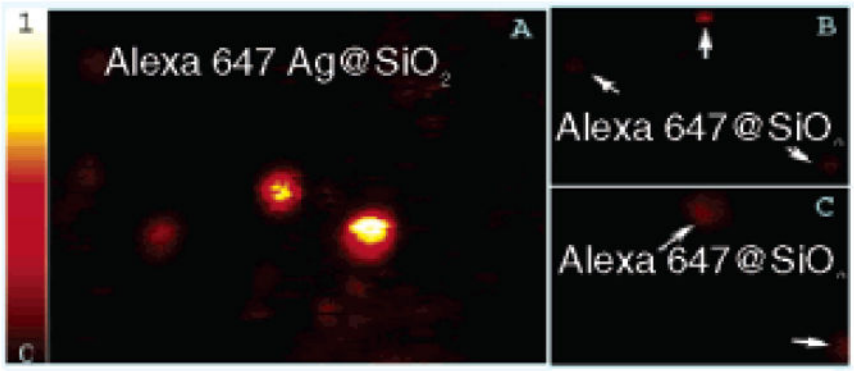

Figure 3.

Scanning confocal images (20 μm × 20 μm) of (A) Alexa 647 Ag@SiO_2, (B) Alexa 647@SiO_2, (C) zoomed in version of that shown in panel B. Intensity counts in the scale were normalized to 1.